Porous Cellulose Aerogels with High Mechanical Performance and their Absorption Behaviors

Manman Xu,[a] Weiqi Bao,[a] Shouping Xu,[c,*] Xiaohui Wang,[a,*] and Runcang Sun [b]

Porous cellulose aerogel materials are attracting increasing interest due to their promising potential in multiple fields. In this paper, highly porous and mechanically strong cellulose aerogels were successfully prepared from microcrystalline cellulose and dissolving pulp in ionic liquid BmimCl *via* a sol–gel polymerization method. The surface morphology and physical properties were characterized by scanning electron microscopy, X-ray diffraction, and compression tests, *etc.* The differences in microstructure, crystalline structure, and mechanical performance of these two kinds of cellulose aerogels were studied and compared. Moreover, the two cellulose aerogels were used as adsorbents to remove dye, oil, and organic solvents. The kinetics and equilibrium capacity were investigated. Results indicate that the cellulose aerogels with high degrees of polymerization have much better mechanical strength and adsorption properties than the cellulose aerogels with low degrees of polymerization.

Contact information: a: State Key Laboratory of Pulp and Paper Engineering, School of Light Industry and Food Science, South China University of Technology, Guangzhou, 510640, China; b: Institute of Biomass Chemistry and Technology, Beijing Forestry University, Beijing, 100083, China; c: School of Chemistry and Chemical Engineering, South China University of Technology, Guangzhou, 510640, China; *Corresponding authors: fewangxh@scut.edu.cn

INTRODUCTION

Aerogels, an important kind of porous material, have been defined as solids having nano-scale pores formed by replacement of liquid in a hydrogel or alcogel with gas (Sehaqui *et al.* 2011). Aerogels typically display high porosities of up to 99%, and high surface areas usually between 100 and 1000 m^2 g^{-1} (Mukhopadhyay and Rao 2008). As ultra-light materials, aerogels have been used in a wide range of applications (Tsioptsias *et al.* 2008; Aaltonen and Jauhiainen 2009). To date, in response to the growing need for sustainable and environmental development, the utilization of naturally occurring polymers is becoming increasingly attractive and important. Natural polymers, *e.g.* chitosan (Ricci *et al.* 2010), alginate (Escudero *et al.* 2009), and cellulose (Wang *et al.* 2012), are promising materials for preparing aerogels due to their excellent biodegradability, hydrophilicity, biocompatibility, low toxicity, and ready availability from renewable resources. In the past a few decades, aerogels from natural polysaccharides have been intensively studied and applied in food, wastewater treatment, sensing, wound dressing, and the pharmaceutical industry (Valentin *et al.* 2006; Chang *et al.* 2008; Surapolchai and Schiraldi 2010) .

Cellulose, the most abundant natural polysaccharide in the world (Moon *et al.* 2011), possess unique properties such as nontoxicity, recyclability, and low cost (Guo *et al.* 2012). As a promising green, inexpensive, and sustainable material to replace the petrochemical derived materials, cellulose is attracting increasing attention. However, cellulose is difficult

to process in most solvents because of its insolubility, which results from the strong intra- and inter-molecular hydrogen bonding. Luckily, an innovative class of green solvents-ionic liquids with excellent dissolving capability, recyclability, and negligible vapor pressure have been developed as the alternative and effective solvent for cellulose processing (Hao *et al*. 2009; Pinkert *et al*. 2009). For example, ionic liquids with imidazolium structure, 1-butyl-3-methylimidazolium chloride (BmimCl) (Liebert and Heinze 2008) have been used to dissolve and process cellulose into hydrogels and the corresponding aerogels. Tsioptsias *et al*. (2008) used 1-allyl-3-methylimidazolium chloride for the cellulose dissolution. Cellulose aerogels were obtained with a BET surface area of 315 m^2 g^{-1}. They also used rapid decompression of the supercritical CO_2 to foam the materials. Aaltonen and Jauhiainen (2009) used 1-butyl-3-methylimidazolium chloride for cellulose dissolution, and regenerated it in aqueous ethanol baths. They obtained a cellulose aerogel with a BET surface area of 539 m^2 g^{-1} by CO_2 supercritical drying. However, most of the aerogels suffer from a lack of mechanical performance, which has limited their further applications. Therefore, an easier and low-cost way to prepare high performance cellulose aerogels is still desired. Moreover, the properties of the cellulose aerogels reported by different groups show great difference, and the effect of raw materials on the properties of cellulose aerogels is unclear.

In this study, two kinds of cellulose aerogels were prepared with microcrystalline cellulose (MCC) and dissolving pulp cellulose (DMCC) by simply regenerating them from their BmimCl ionic liquid (IL) solution using ethanol as a coagulant, and freeze drying them afterwards. The structure and properties of the two cellulose aerogels derived from different raw materials were analyzed and compared in detail. Furthermore, the two cellulose aerogels were studied as adsorbents to remove dye and organic solvents. The absorption kinetics and equilibrium capacity were also investigated. This study presents the possibility to gain functional cellulose aerogels with perfect network structure in a simple and inexpensive preparation. Investigation into the absorption behaviors of cellulose aerogels derived from different raw materials also provides useful information for the application of cellulose-based aerogel as absorption materials.

EXPERIMENTAL

Materials

Microcrystalline cellulose (MCC) with a polymerization degree of 280 was supplied by Sinopharm Chemical Reagent Co., Ltd. Dissolving pulp cellulose (DMCC) with a polymerization degree of 884 was supplied by Shandong Bohi Industry Co., Ltd. A whole piece of pulp board was cut into shreds, fed into the shredder, and ball-milled into powder before use. 1-Butyl-3-methylimidazolium chloride (BmimCl) was from Shanghai Chengjie Chemical Co., Ltd. The dye, rhodamine 6G, was from Aladdin Chemistry Co., Ltd of China, and it was used as received without further purification.

Preparation of Cellulose Alcogels and Aerogels

20 g of ionic liquid was dissolved in a 50 mL three-necked round-bottomed flask in an oil bath at 110 °C under the protection of nitrogen. Then, the desired amount (0.6, 0.8, 1.0 or 1.2 g) of MCC (or DMCC) was slowly added to the solvent and stirred with magnetic stirring for 4 to 6 h at 110 °C to obtain a transparent cellulose solution (3 to 6 wt%). The solution was decanted into lubricated watch glasses (50 mm diameter, 30 mm height) to

give a 10-mm-thick layer, and degassed by ultrasound (100 W, 60 °C). The resulting solution was immersed into an ethanol coagulation (regeneration) bath at ambient temperature, until detected by 0.1 mol/L $AgNO_3$ solution without sediment. The regenerated cellulose alcogel was washed with several changes of ultrapure water to remove residual ethanol, which fulfilled the solvent exchange.

The obtained cellulose alcogel was precooled in refrigerator at 0 °C for 12 h. After that, it was freeze-dried to obtain the cellulose aerogel.

Characterization

Scanning electron microscopy

After frozen brittle failure, scanning electron microscopy (SEM) observation of the surfaces and cross section of cellulose aerogels was carried out using a Hitachi S-4800 microscope (Hitachi Limited, Japan).

X-ray diffractometry

The X-ray diffraction (XRD) of cellulose aerogel and cellulose was determined by a D/max-IIIA X-ray diffractometer (Bruker Corporation, Germany), in which the high-intensity monochromatic nickel-filtered Cu Kα radiation ($\lambda = 0.15418$ nm) was generated at 40 kV and 40 mA. Samples were scanned at a speed of 1°/min, ranging from $2\theta = 5$ to 50° with step size of 0.02° at room temperature.

Mechanical properties

The compression strength of the aerogels was measured on an Instron Universal Testing Machine 5565 (Norwood Corporation, USA) with a load cell of 2000 N. Before testing, the aerogels were tailored to the same size of 10 mm in length, and the strain rate of 10 mm/min was applied.

Adsorption isotherm

To evaluate the equilibrium adsorption isotherm of cellulose aerogel, rhodamine 6G was used as the adsorbate. A serial dilution of rhodamine 6G was prepared in aqueous solutions at various concentrations ranging from 5 to 30 mg/L. Subsequently, 0.1 g cellulose aerogel and 10 mL rhodamine 6G solution with desired concentration were transferred into a 25 mL conical flask and shaken using an incubator shaker at different temperatures for 24 h.

Kinetic adsorption

Briefly, 0.1 g MCC aerogel or DMCC aerogel was added into 10 mL rhodamine 6G solution at an initial concentration of 10 mg/L and placed into a 25 mL conical flask at a constant temperature of 25 °C. Then the solution was carefully withdrawn from the conical flask to be conducted absorbance detection by the ultraviolet spectrophotometer at determined time intervals.

Effect of cellulose

0.1 g MCC aerogel or DMCC aerogel was added into 10 mL 10 mg/L rhodamine solution and shaken in the constant temperature water-bath oscillator for 24 h, respectively. The absorbance of the residual solution was measured by a UV/VIS spectrophotometer (TUH810 SPC, from Beijing Pgeneral Co., Ltd) at a maximum wavelength of 528 nm. The

final concentration of the solution was calculated according to a calibration curve. The dye adsorption capacity at equilibrium, q_e (mg/g), can be calculated from Eq. 1,

$$q_e = \frac{V(C_0 - C_e)}{m} \tag{1}$$

where C_0 (mg/L) is the initial concentration of rhodamine 6G in liquid phase, C_e (mg/L) is the concentration of rhodamine 6G in liquid phase at equilibrium, V (L) is the total volume of rhodamine 6G solution, and m (g) is the mass of cellulose aerogel.

Organic solvent adsorption

The adsorption of cellulose aerogel on cyclohexane, toluene, gasoline, liquid paraffin, vegetable oil, and carbon tetrachloride was evaluated in this experiment. Similarly, 0.1 g DMCC aerogel was added into the organic solvent, and all the other procedures were unchanged, as mentioned above.

RESULTS AND DISSCUSSION

Preparation of Cellulose Aerogel

Figure 1 is the schematic presentation of the preparation of cellulose aerogels. As shown, in general the cellulose aerogel was prepared by regeneration of the cellulose from its ILs solution and then the resulting regenerated cellulose alcogel was freeze dried.
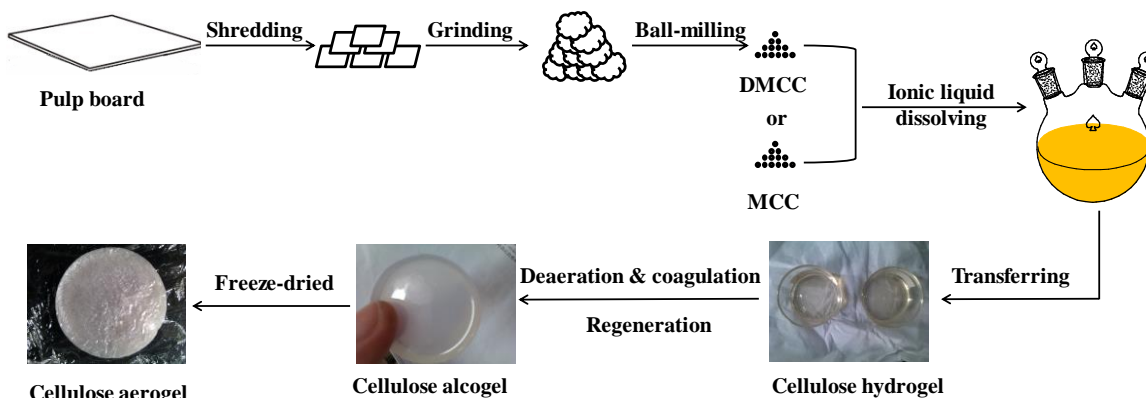

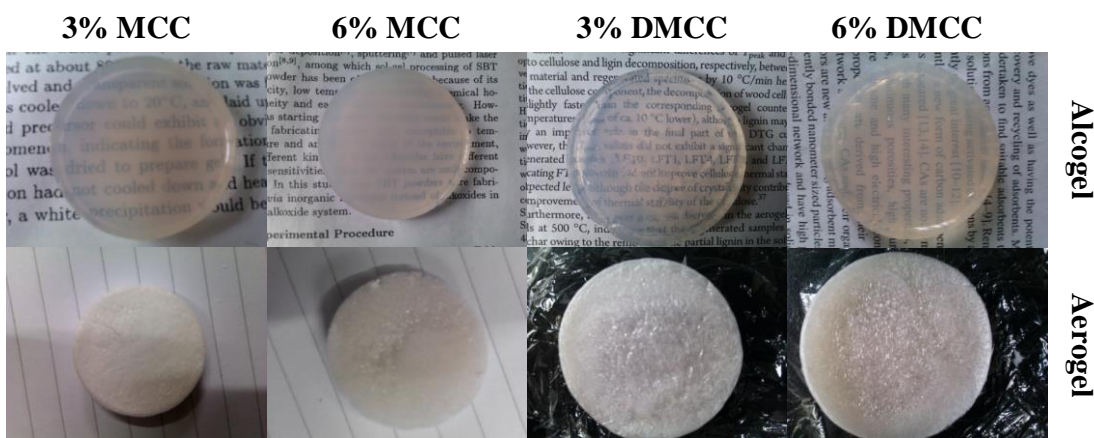**Fig. 1.** Schematic presentation of cellulose aerogel preparation

Fig. 2. Photographs of cellulose alcogels and aerogels

Two different raw materials including MCC and DMCC obtained by shredding, grinding and ball-milling of pulp board were used to prepare cellulose alcogel and aerogel. The images of cellulose alcogels and aerogels are shown in Fig. 2. It can be seen that the cellulose alcogels exhibited good transparency. With the same thickness, the transparency of cellulose alcogels decreased with increasing cellulose content. With the same content of cellulose, DMCC alcogel was more transparent than MCC alcogel. The cellulose aerogel was very light and appeared as a white lump with a rough surface.

## Microscopic Morphology of Cellulose Aerogel

Figure 3 shows the SEM images of cellulose aerogels. The aerogels obtained by MCC and DMCC showed differences in morphology between the surface and cross sections. The images of MCC aerogels in Fig. 3A and B show a dense surface, whereas DMCC aerogels display a macroporous structure. It can be observed that the inner parts of all the aerogel samples viewed on the cross sections displayed more uniform, nanometer-sized pore structures composed of fibrillar networks (Figure 3E, F, G, and H).
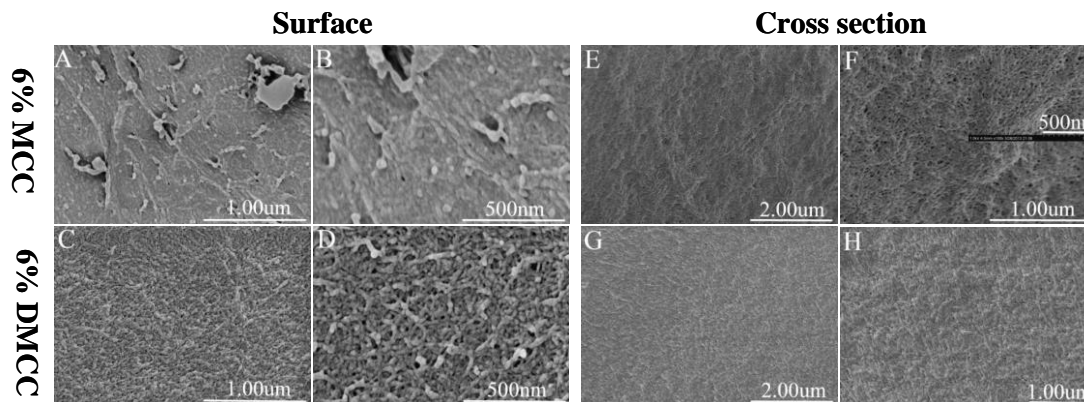
Fig. 3. SEM images of cellulose aerogels. A,B,E, and F are Images of 6% MCC aerogel; C,D,G, and H are images of 6% DMCC aerogel; A through D are high-magnification images of the surface; E through H are high-magnification images of the cross section of the aerogels.

XRD Analysis

Powder X-ray diffraction was used to probe the crystallinity of the cellulose raw materials and the corresponding cellulose aerogels (Fig. 4).
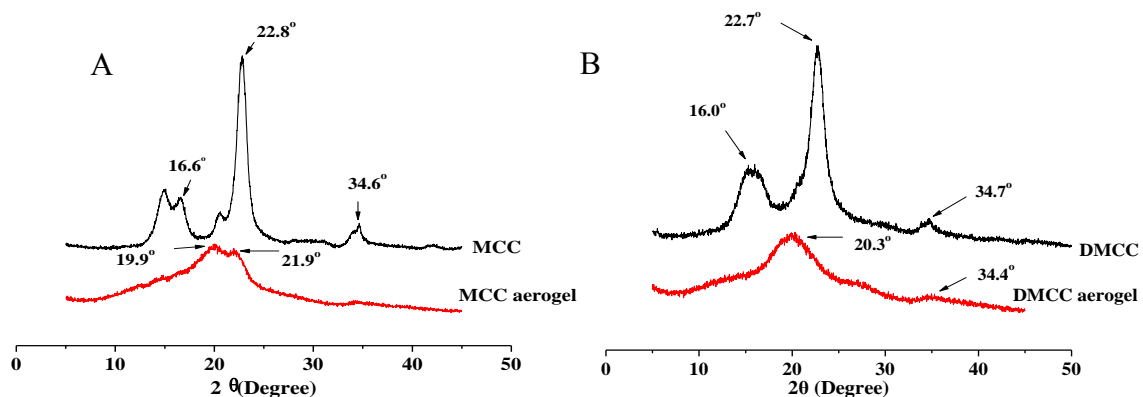

Fig. 4. A) XRD patterns of MCC and 6% MCC aerogel. B) XRD patterns of DMCC and 6% DMCC aerogel

The original MCC showed peaks at around 16.6°, 22.8°, and 34.6°, which represented cellulose I crystalline structure. However, the peak at 16.6° of the 6% MCC aerogel disappeared, and a peak at 19.9° appeared. This indicated that the crystalline structure of MCC aerogel changed from cellulose I into cellulose II and part of the crystalline region turned into an amorphous region (Zhang *et al*. 2005; Zhao *et al*. 2007). At the same time, the diffraction intensity of the new peak had shown a significant drop, which means a drop of cellulose crystallinity in MCC aerogel. The cellulose crystallinity degree in 6% DMCC aerogel also decreased.

Mechanical Properties

The mechanical properties of cellulose aerogels were explored. The curves of stress-strain from uniaxial compression of different concentration of MCC and DMCC aerogels are exhibited in the Fig. 5. It can be seen that both curves of MCC and DMCC aerogels presented a linear slope at the initial stage, which was indicative of the elastic behavior of the aerogel samples for small strain values. At the high strain region, the compress stress increased with the strain. The maximum Young's modulus appeared in the 5% MCC aerogel and 4% DMCC aerogel, and Young's modulus of 5% MCC aerogel was lower than that of 4% DMCC aerogel. This means that the network structure is more complex and compact in DMCC aerogels. Although the concentration was lower than that of MCC aerogel, the extra cellulose cannot support the strength in the porous structure of aerogels, which stated that the polymerization degree plays a more important role in the mechanical strength of aerogels.
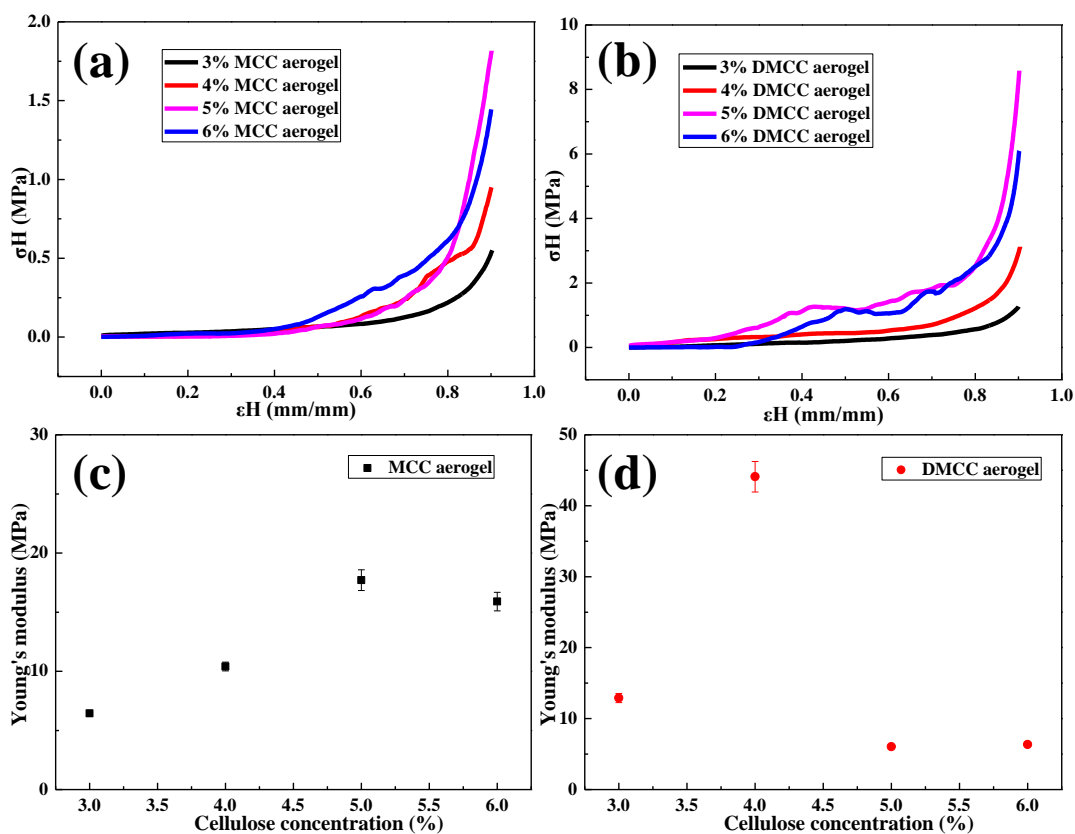
Fig. 5. Compressive stress–strain curves of MCC (a) and DMCC (b), (c, d) Young's modulus of MCC and DMCC with different contents of cellulose

Adsorption Properties

The highly porous and interconnected three-dimensional structure of the cellulose aerogel makes it a good adsorbent. Moreover, there are a lot of hydroxyl groups in the cellulose aerogels, which tend to form hydrogen bonds with the nitrogen and oxygen atoms in the rhodamine 6G molecule. Therefore, rhodamine 6G molecules can get into the network structure of cellulose aerogels, and be adsorbed on the surface due to the attraction of hydrogen bonds. Figure 6(a) gives the visual illustration for the removal of rhodamine dye by cellulose aerogel. It was found that the Rhodamine 6G adsorbed well on the aerogel.
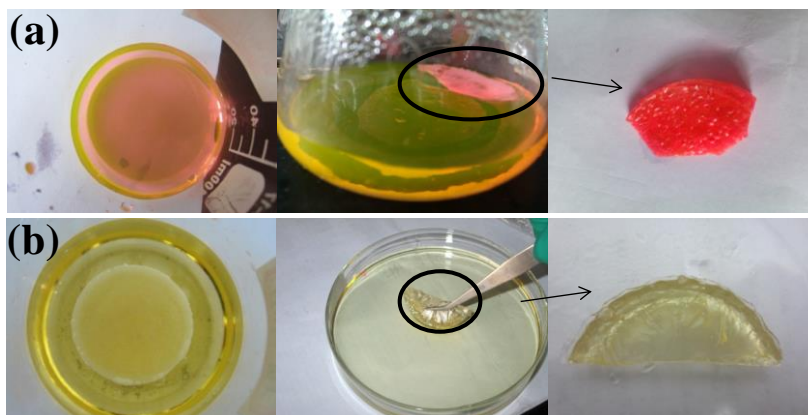
Fig. 6. Images of adsorption of rhodamine 6G (a) and organic solvent (b) on cellulose aerogels

Adsorption Isotherm

Adsorption isotherms of rhodamine 6G is shown in Fig.7a The adsorption of rhodamine 6G increased with temperature from 30 to 40 °C, which presents an endothermic process. According to Langmuir and Freundlich isotherms, the data will be fitted to the models of Langmuir and Freundlich.
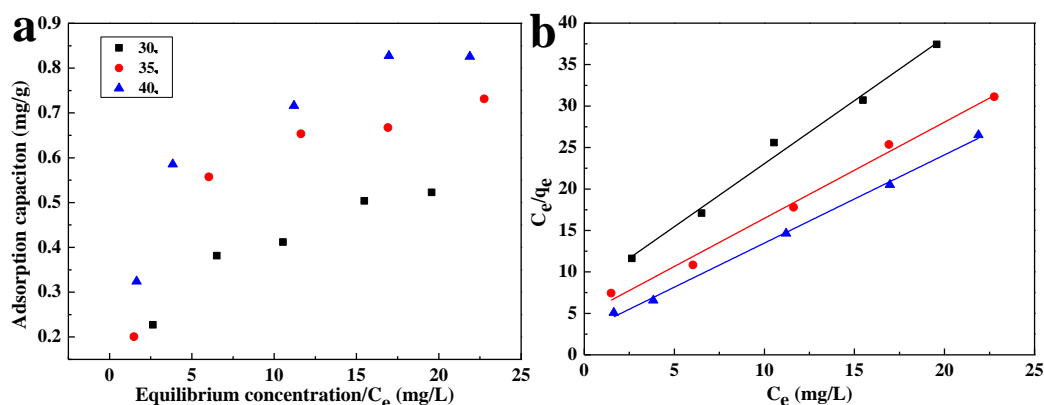
Fig. 7. (a) Adsorption isotherms of 6% DMCC aerogel. (b) Langmuir plots for adsorption of rhodamine 6G dye on 6% DMCC aerogel

The Langmuir isotherm is based upon the hypothesis of three conditions that adsorption takes place at monomolecular layer, the solid surface is uniform, and there is no interaction among adsorbates. The linearized Langmuir isotherm equation is as follows (Langmuir 1918; Eq. 2),

$$\frac{C_e}{q_e} = \frac{1}{q_0 b} + \frac{C_e}{q_0} \tag{2}$$

***bioresources*.com**

where q_e (mg/g) is the adsorption capacity, C_e (mg/L) is the equilibrium concentration of solute, q_o (mg/g) is the maximum capacity of adsorbate to form a complete monolayer on the surface, and b (L/mg) is the Langmuir constant related to the heat of adsorption. Using C_e/q_e as the x-axis and C_e as the y-axis, the data can be linearly fitted (Fig. 7b), through which q_o and b can be calculated from the slope and the intercept respectively.

Table 1. Isotherm Parameters for Removal of Rhodamine 6G Dye by Cellulose Aerogel

Temperature (°C)	Langmuir constants		
	R^2	q_0 (mg/g)	b (L/mg)
30	0.9908	0.6579	0.1935
35	0.9901	0.8618	0.2390
40	0.9973	0.9403	0.3740

Values of R^2, q_o, and b are presented in Table 1. The adsorption capability increased with *b* value, which increased with temperature, illustrating that the adsorption of rhodamine 6G on DMCC aerogels increased with temperature. This result implied that the affinity of the binding sites for rhodamine 6G increased with the temperature. It is widely known that micropores play a leading role in material transportation providing most of the active adsorption sites. Thus, the increased micropores during the formation of DMCC aerogels can largely improve the adsorption capability. However, the experimental adsorption capacity (q_e) was less than the maximum adsorption capacities, which is probably due to some unoccupied concentration. The R^2 value of Langmuir model exceeded 0.99, indicating that this model closely matched the experimental data.

The main characteristics of the Langmuir isotherm can be described by R_L, a dimensionless constant, which determines the isotherm of the adsorption process by Eq. 3 (Sakkayawong *et al.* 2005),

$$R_L = \frac{1}{(1+bC_0)} \tag{3}$$

where b is the Langmuir constant, C_o is the initial concentration of rhodamine 6G (mg/L), and R_L values indicate the type of adsorption isotherm, which can be either unfavorable ($R_L>1$), linear ($R_L=1$), favorable ($0<R_L<1$), or irreversible ($R_L=0$). All values of R_L calculated in the experiment were in the range of 0.9901 to 0.9990 according to the equation (5), illustrating that the adsorption process is favorable for DMCC aerogels.

Adsorption Kinetic Considerations

Using adsorption time as the x-axis and adsorption capacity as the y-axis, the influence of adsorption time on adsorption capacity of MCC and DMCC aerogels are shown in Fig. 9(a). The adsorption of rhodamine 6G on aerogels contains three stages: the first one is that rhodamine 6G diffused to the surface of aerogels and is adsorbed by the molecules on the surface. The second one is that rhodamine 6G gets into the porous network structure through the solution and is adsorbed rapidly until saturation, and the last state is the saturation state. For MCC aerogels, the three stages were 0 to 20 min, 20 to 60 min, and after 60 min, respectively, while those of DMCC aerogels were 0 to 30 min, 30 to 120 min and after 120min. These findings corresponded with the liquid phase adsorption principle of porous adsorbent theoretically. Kinetic data deal with the pseudo-second-order kinetic model, in which the plot of t/q_t versus t shows a linear relationship and can be expressed as (Eq. 4),

$$\frac{t}{q_t} = \frac{1}{k_2 q_e^2} + \frac{1}{q_e} t \tag{4}$$

where q_e is equilibrium adsorption capacity, and k_2 is the second-order constant, which can be determined from the slope and intercept of plot t/q_t versus t (Fig. 8b) and shown in Table 2. It shows a good agreement with experimental data with the pseudo-second-order kinetic model.
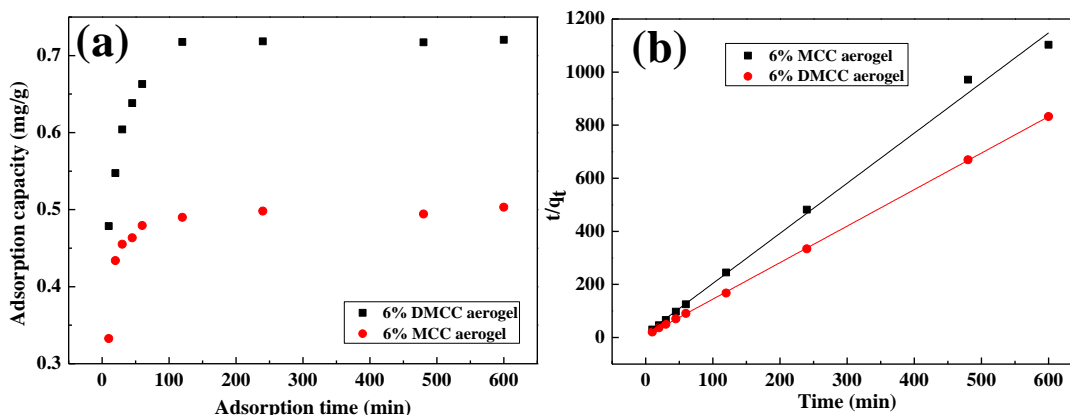
Fig. 8. (a) Equilibrium curves for adsorption of rhodamine 6G dye onto cellulose aerogels. (b) Pseudo-second-order kinetics for adsorption of rhodamine 6G dye on cellulose aerogels

Table 2. Pseudo-Second-Order Adsorption Rate Constants, Calculated and Experimental q_e Values for Adsorption of Rhodamine 6G on Cellulose

Aerogel	q_e (exp)(mg/g)	k_2 (g/mg min)	q_e (cal)(mg/g)	R^2
6% MCC	0.5045	0.5406	0.5032	0.9999
6% DMCC	0.7223	0.2675	0.7269	0.9999

The adsorption process of rhodamine 6G can be summarized as: diffusion stage outside the particle (membrane diffusion), pore diffusion stage, and adsorption reaction stage. According to the theory of adsorption kinetics, the adsorption rate is mainly determined by the first and second stage, between which the slower one controls the adsorption velocity.

The diffusion model inside the particle can be expressed as (Eq. 5),

$$\log(1 - F^2) = kT/2.303 \tag{5}$$

and the liquid film diffusion model can be expressed as (Eq. 6),

$$\ln(1 - F) = -Kt \tag{6}$$

where $F = q_t/q_e$, and K is the rate constant. The linear fit –log $(1-F^2)$ and ln $(1-F)$ versus time, respectively (Fig. 9), and the fitted equations and models are shown in Table 3.

Table 3. Diffusion Model Rate Constants

| Aerogel	Liquid film diffusion		Intraparticle diffusion	
	K	R^2	K	R^2
6% MCC	0.0340	0.8501	0.0314	0.8702
6% DMCC	0.0281	0.9821	0.0254	0.9878
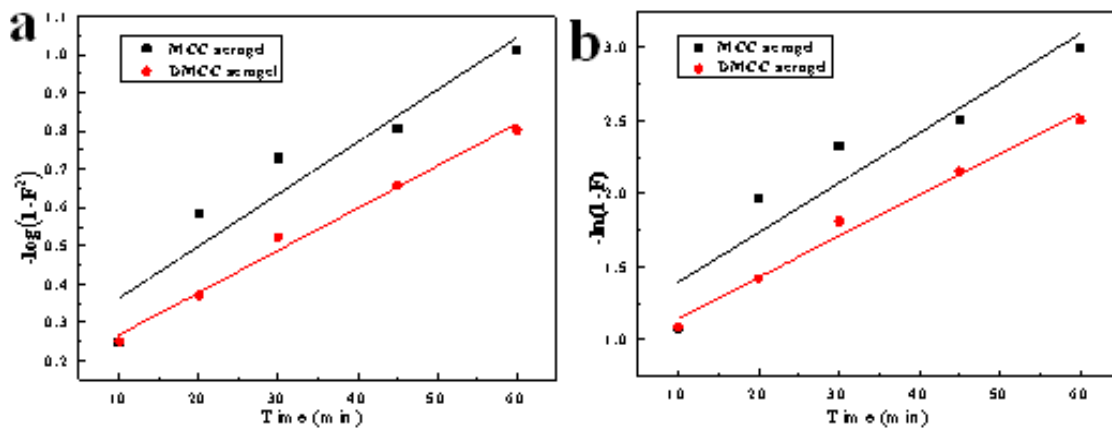
Fig. 9. a) Intraparticle diffusion model, and b) liquid film diffusion model of 6% MCC and 6% DMCC aerogels

Table 3 shows that a better linear relation is obtained with the DMCC aerogels. However, all the fitted lines failed to pass through the origin of the graph, which indicates that the processes of diffusion inside the particle and liquid membrane diffusion influenced the adsorption on cellulose aerogels. The adsorption process was determined by their combined effects.

Effect of Raw Materials on the Adsorption Capability

From the above study, the structure and diffusion of pores inside aerogels are varied depending on the types of cellulose with different polymerization degree. The different adsorption capacities of rhodamine 6G on aerogels are shown in Fig. 10.
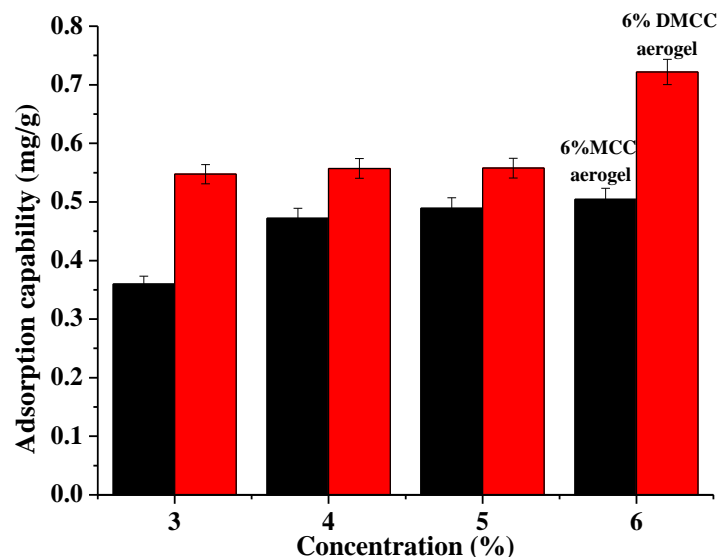

Fig. 10. The influence of cellulose on adsorption capability of rhodamine 6G

Figure 10 shows that the adsorption capacity increased with the concentration of cellulose. For the same concentration, the adsorption capacity of DMCC aerogels was higher than MCC aerogels. The adsorption capacity increased with the increasing density of aerogels, and the density of aerogels increased with the increasing concentration of cellulose.

Adsorption of Oil and Organic Solvents

In this experiment, 0.1 g 6% DMCC aerogels was used to adsorb oil and organic solvents. As shown in Fig. 6 (b), the aerogels became transparent and hard after adsorption, and the adsorption efficiencies are presented in Fig. 11.
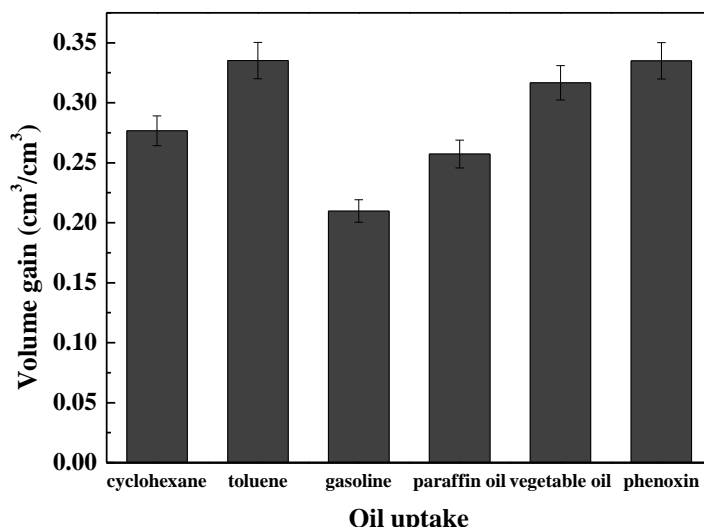
Fig. 11. Adsorption capacities of the DMCC aerogels for a range of organic solvents and oils in terms of its volume gain

When the aerogels were immersed into the liquid, they immediately started to adsorb the organic compound and turned transparent immediately. After 24 h adsorption, the aerogel got hard gradually. Measuring the weight of aerogels after 24 h, the adsorption volume can be calculated from density. From the data, the maximum adsorption volume was obtained, and it reached 10 times that of the aerogel. When the organic solution was colored, such as gasoline, the aerogel gained the same color with the solution during the adsorption process. However, after the solution that had been adsorbed inside the aerogel had become volatilized, the colored matter remained in the aerogel, and this darkened the aerogel. The mechanism remains to be discovered.

CONCLUSIONS

1. Cellulose aerogels were successfully fabricated by a sol–gel polymerization method by using microcrystalline cellulose and dissolving pulp as raw materials in ionic liquids BmimCl.

2. The prepared cellulose aerogels were found to have high surface reactivity, extra-high porosity, and highly mechanical properties. The highest Young's modulus was observed in the 5% MCC aerogel and the 4% DMCC aerogel.

3. The ability of cellulose aerogels to adsorption rhodamine 6G and organic compounds was tested using equilibrium, kinetics, and the adsorption experiments, which confirmed cellulose aerogels to be effective adsorbents for the adsorption of rhodamine 6G and organic compounds. The good adsorption ability towards rhodamine 6G and some organic compounds would make cellulose aerogels a viable candidate for efficient absorbents for the purposes of storage, clean-up, and the safe disposal of organic pollutants.

ACKNOWLEDGMENTS

REFERENCES CITED

Aaltonen, O., and Jauhiainen, O. (2009). "The preparation of lignocellulosic aerogels from ionic liquid solutions," *Carbohydrate Polymers* 75(1), 125-129. DOI: 10.1016/j.carbpol.2008.07.008

Chang, X., Chen, D., and Jiao, X. (2008). "Chitosan-based aerogels with high adsorption performance," *The Journal of Physical Chemistry B* 112(26), 7721-7725. DOI: 10.1021/jp8011359

Escudero, R. R., Robitzer, M., Di Renzo, F., and Quignard, F. (2009). "Alginate aerogels as adsorbents of polar molecules from liquid hydrocarbons: Hexanol as probe molecule," *Carbohydrate Polymers* 75(1), 52-57. DOI: 10.1016/j.carbpol.2008.06.008

Guo, Y., Wang, X., Shu, X., Shen, Z., and Sun, R.-C. (2012). "Self-assembly and paclitaxel loading capacity of cellulose-graft-poly (lactide) nanomicelles," *Journal of Agricultural and Food Chemistry* 60(15), 3900-3908. DOI: 10.1021/jf3001873

Hao, Y., Peng, J., Li, J., Zhai, M., and Wei, G. (2009). "An ionic liquid as reaction media for radiation-induced grafting of thermosensitive poly (< i> N</i>-isopropylacrylamide) onto microcrystalline cellulose," *Carbohydrate Polymers* 77(4), 779-784. DOI: 10.1016/j.carbpol.2009.02.025

Langmuir, I. (1918). "The adsorption of gases on plane surfaces of glass, mica and platinum," *Journal of the American Chemical Society* 40(9), 1361-1403. DOI: 10.1021/ja02242a004

Liebert, T., and Heinze, T. (2008). "Interaction of ionic liquids with polysaccharides. 5. Solvents and reaction media for the modification of cellulose," *BioResources* 3(2), 576-601.

Moon, R. J., Martini, A., Nairn, J., Simonsen, J., and Youngblood, J. (2011). "Cellulose nanomaterials review: Structure, properties and nanocomposites," *Chemical Society Reviews* 40(7), 3941-3994. DOI: 10.1039/C0CS00108B

Mukhopadhyay, M., and Rao, B. S. (2008). "Modeling of supercritical drying of ethanol‐Soaked silica aerogels with carbon dioxide," *Journal of Chemical Technology and Biotechnology* 83(8), 1101-1109. DOI: 10.1002/jctb

Pinkert, A., Marsh, K. N., Pang, S., and Staiger, M. P. (2009). "Ionic liquids and their interaction with cellulose," *Chemical Reviews* 109(12), 6712-6728. DOI: 10.1021/cr9001947

Ricci, A., Bernardi, L., Gioia, C., Vierucci, S., Robitzer, M., and Quignard, F. (2010). "Chitosan aerogel: A recyclable, heterogeneous organocatalyst for the asymmetric direct aldol reaction in water," *Chemical Communications* 46(34), 6288-6290. DOI: 10.1039/c0cc01502d

Sakkayawong, N., Thiravetyan, P., and Nakbanpote, W. (2005). "Adsorption mechanism of synthetic reactive dye wastewater by chitosan," *Journal of Colloid and Interface Science* 286(1), 36-42. DOI: 10.1016/j.jcis.2005.01.020

Sehaqui, H., Zhou, Q., and Berglund, L. A. (2011). "High-porosity aerogels of high specific surface area prepared from nanofibrillated cellulose (NFC)," *Composites Science and Technology* 71(13), 1593-1599. DOI: 10.1016/j.compscitech.2011.07.003

Surapolchai, W., and Schiraldi, D. A. (2010). "The effects of physical and chemical interactions in the formation of cellulose aerogels," *Polymer bulletin* 65(9), 951-960. DOI: 10.1007/s00289-010-0306-x

Tsioptsias, C., Stefopoulos, A., Kokkinomalis, I., Papadopoulou, L., and Panayiotou, C. (2008). "Development of micro-and nano-porous composite materials by processing cellulose with ionic liquids and supercritical CO_2," *Green Chemistry* 10(9), 965-971. DOI: 10.1039/b803869d

Valentin, R., Horga, R., Bonelli, B., Garrone, E., Di Renzo, F., and Quignard, F. (2006). "FTIR spectroscopy of NH3 on acidic and ionotropic alginate aerogels," *Biomacromolecules* 7(3), 877-882. DOI: 10.1021/bm050559x

Wang, Z., Liu, S., Matsumoto, Y., and Kuga, S. (2012). "Cellulose gel and aerogel from LiCl/DMSO solution," *Cellulose* 19(2), 393-399. DOI: 10.1007/s10570-012-9651-2

Zhang, H., Wu, J., Zhang, J., and He, J. (2005). "1-Allyl-3-methylimidazolium chloride room temperature ionic liquid: a new and powerful nonderivatizing solvent for cellulose," *Macromolecules* 38(20), 8272-8277. DOI: 10.1021/ma0505676

Zhao, H., Kwak, J. H., Conrad Zhang, Z., Brown, H. M., Arey, B. W., and Holladay, J. E. (2007). "Studying cellulose fiber structure by SEM, XRD, NMR and acid hydrolysis," *Carbohydrate Polymers* 68(2), 235-241. DOI: 10.1016/j.carbpol.2006.12.013